Acta Crystallographica Section F
Structural Biology and Crystallization Communications
ISSN 1744-3091

Complex structure of a bacterial class 2 histone deacetylase homologue with a trifluoromethylketone inhibitor

Tine Kragh Nielsen,[a]‡ Christian Hildmann,[b] Daniel Riester,[b] Dennis Wegener,[b] Andreas Schwienhorst[b] and Ralf Ficner[a]*

[a]Abteilung für Molekulare Strukturbiologie, Institut für Mikrobiologie und Genetik and GZMB, Justus-von-Liebig Weg 11, 37077 Göttingen, Germany, and [b]Abteilung für Molekulare Genetik und Präparative Molekularbiologie, Institut für Mikrobiologie und Genetik, Grisebachstrasse 8, 37077 Göttingen, Germany

‡ Present address: Ontario Cancer Institute, TMDT, 101 College Street, Rm. 4-601, Toronto, Ontario M5G 1L7, Canada.

Correspondence e-mail: rficner@gwdg.de

Received 30 November 2006
Accepted 15 March 2007

PDB Reference: histone deacetylase homologue–trifluoromethylketone inhibitor complex, 2gh6, r2gh6sf.

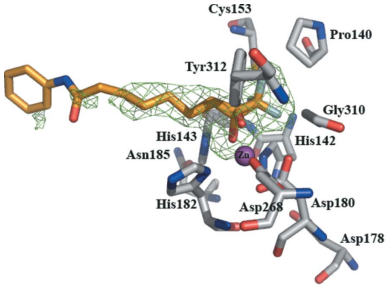

Histone deacetylases (HDACs) have emerged as attractive targets in anticancer drug development. To date, a number of HDAC inhibitors have been developed and most of them are hydroxamic acid derivatives, typified by suberoylanilide hydroxamic acid (SAHA). Not surprisingly, structural information that can greatly enhance the design of novel HDAC inhibitors is so far only available for hydroxamic acids in complex with HDAC or HDAC-like enzymes. Here, the first structure of an enzyme complex with a nonhydroxamate HDAC inhibitor is presented. The structure of the trifluoromethyl ketone inhibitor 9,9,9-trifluoro-8-oxo-*N*-phenylnonanamide in complex with bacterial FB188 HDAH (histone deacetylase-like amidohydrolase from *Bordetella*/*Alcaligenes* strain FB188) has been determined. HDAH reveals high sequential and functional homology to human class 2 HDACs and a high structural homology to human class 1 HDACs. Comparison with the structure of HDAH in complex with SAHA reveals that the two inhibitors superimpose well. However, significant differences in binding to the active site of HDAH were observed. In the presented structure the O atom of the trifluoromethyl ketone moiety is within binding distance of the Zn atom of the enzyme and the F atoms participate in interactions with the enzyme, thereby involving more amino acids in enzyme–inhibitor binding.

1. Introduction

Histone deacetylase (HDAC) inhibitors are a promising new class of anticancer compounds that target key steps of tumour development. They exhibit antiproliferative activities (Bouchain & Delorme, 2003), induce differentiation and/or apoptosis (Marks *et al.*, 2000) and show potent antimetastatic (Liu *et al.*, 2003) and antiangiogenic (Qian *et al.*, 2006) properties. Furthermore, clinical trials indicate that HDAC inhibitors are well tolerated and exhibit clinical activity against a large number of human malignancies (Johnstone, 2002; Rosato & Grant, 2003; Villar-Garea & Esteller, 2004). Very recently, the first HDAC inhibitor (SAHA, Zolina) has been approved for the treatment of cutaneous T-cell lymphoma (CTCL). To date, a variety of HDAC inhibitors from various structural classes have been discovered (Monneret, 2005). Structural information on inhibitor–enzyme complexes, however, is only available for hydroxamic acids, *e.g.* suberoyl anilide hydroxamic acid (SAHA) or trichostatin A (TSA) (Finnin *et al.*, 1999; Vannini *et al.*, 2004; Somoza *et al.*, 2004; Nielsen *et al.*, 2005). Thus, structure-based design and molecular modelling studies are still rather limited.

Here, we describe the first crystal structure of a nonhydroxamate HDAC inhibitor in complex with a bacterial class 2 HDAC homologue, FB188 HDAH (Hildmann *et al.*, 2004), which serves as a good model for class 2 HDACs (Nielsen *et al.*, 2005; Riester *et al.*, 2004). The HDAC inhibitor (Wada *et al.*, 2003) belongs to the class of trifluoromethyl ketones that has previously been reported to comprise potent inhibitors not only of HDACs but also of enzymes as diverse as human neutrophil elastase (Cowan *et al.*, 2000), phospholipases (Koutek *et al.*, 1994) and hormone esterases (Kamita *et al.*, 2003). The structure of the complex is compared with a structure of

Table 1
Data-collection and refinement statistics.

Values in parentheses are for the last shell.

Data collection	
Resolution range (Å)	40–2.21 (2.29–2.21)
Space group	$P2_1$
Unit-cell parameters (Å, °)	a = 68.5, b = 94.9, c = 123.3, β = 104.3
No. of unique reflections	76561
No. of observed reflections	279486
Completeness (%)	99.1 (92.9)
R_{sym}† (%)	6.2 (34.1)
$I/\sigma(I)$	15.3 (3.1)
Refinement statistics	
Resolution range (Å)	39.4–2.2 (2.26–2.21)
R factor‡ (%)	15.8 (20.5)
R_{free}‡ (%)	21.4 (29.4)
Deviations from ideal geometry	
Bond lengths (Å)	0.015
Bond angles (°)	1.559
Ramachandran plot§	
Most favoured (%)	90.6/
Additionally allowed (%)	9.1
Generously allowed (%)	0.3
No. of protein residues	1492
No. of waters	783

† $R_{sym} = 100 \times |I - \langle I\rangle|^2/|I|^2$, where I is the observed intensity and $\langle I\rangle$ is the average intensity for multiple measurements. ‡ R factor $= 100 \times \sum ||F_o| - |F_c||/\sum |F_o|$, where F_o and F_c are the observed and calculated structure factors, respectively. R_{free} is the cross-validation R factor calculated for 5% of the reflections omitted during the refinement process. § Calculated with *PROCHECK* (Laskowski *et al.*, 1993).

FB188 HDAH with a hydroxamate inhibitor, which we recently solved to high resolution (Nielsen *et al.*, 2005).

2. Materials and methods

2.1. Expression, purification, crystallization and structure determination

HDAH was expressed and purified as described previously and crystallized under identical conditions to those reported by Nielsen *et al.* (2005) (see Table 1). The obtained crystals were soaked with the inhibitor added in molar excess directly to the drop for at least 48 h, followed by a quick soak in a cryosolution consisting of the mother liquor with 20% glycerol before mounting the crystals in the X-ray beam. Data were collected to a resolution of 2.21 Å using a rotating-anode generator (see Table 1 for data statistics). The structure was determined by the molecular-replacement method with *MOLREP* (Vagin & Teplyakov, 1997) using the known HDAH structure (PDB code 1zz1) and the energy-minimized structure of the inhibitor (obtained with *PRODRG*; Schüttelkopf & van Aalten, 2004) was fitted into the extra density. There are four molecules in the asymmetric unit. This structure was refined with *REFMAC* (Murshudov *et al.*, 1997) and modelled with *O* (Jones & Kjeldgaard, 1997) until a final R and R_{free} of 15.8% and 21.4%, respectively, were reached. Figs. 1 and 2 were produced using *PyMOL* (DeLano, 2002).

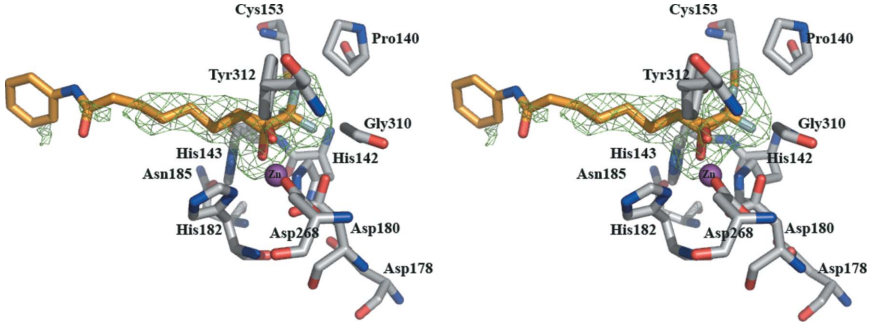

Figure 1
Stereoview of the active site of HDAH with the two different conformations of the O atom in 9,9,9-trifluoro-8-oxo-*N*-phenylnonanamide. The 9,9,9-trifluoro-8-oxo-*N*-phenylnonanamide is shown in orange and the Zn ion in magenta. The electron-density map shown is an $|F_o - F_c|$ OMIT map, which is contoured at 3σ.

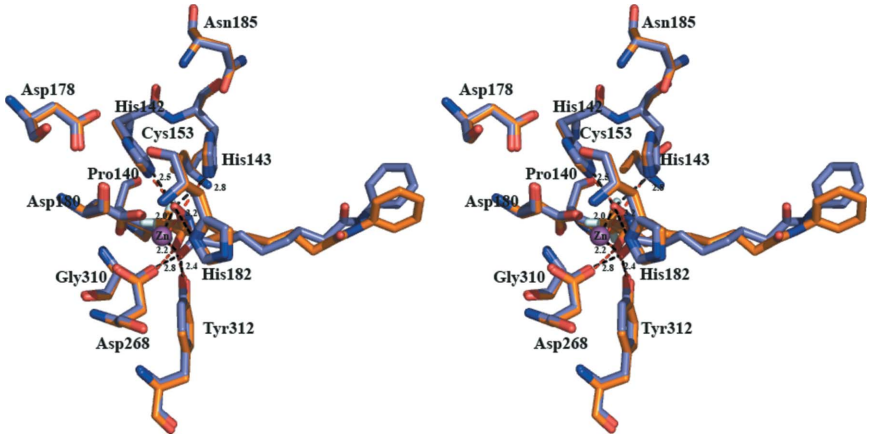

Figure 2
Stereoview of a superposition of the active site with two different inhibitors. The Zn ion is shown as a magenta sphere. The amino acids in the active site are shown in stick mode. The active site of HDAH with 9,9,9-trifluoro-8-oxo-*N*-phenylnonanamide bound is coloured orange and the hydrogen bonds to the two O atoms are shown as red dashes, whilst the active site of HDAH with SAHA bound (PDB code 1zz1) is coloured purple with the hydrogen bonds from the two O atoms shown as black dashes. The distances depicted in the figure are for the SAHA complex (for clarity, only one set of numbers is shown); the corresponding distances for 9,9,9-trifluoro-8-oxo-*N*-phenylnonanamide can be found in Table 2. The hydrogen-bond distances are from one of the molecules in the asymmetric unit; however, the distances found in the other complexes are similar.

Table 2
Overview of the contacts made by the O atom and the three F atoms of the head group in 9,9,9-trifluoro-8-oxo-*N*-phenylnonanamide.

The O atoms are labelled (*A*) or (*B*) to represent the two different conformations adapted by this atom. The contacts in the table are consistent between the four molecules in the asymmetric unit. The distances given are from the *A* molecule and vary less than 1% between the four molecules.

Atom in the inhibitor	Distance (Å)	Contact
O2(*A*)	1.8	Zn
	2.8	Tyr312 OH
	3.0	Asp268 OD2
O2(*B*)	2.1	Zn
	2.8	His143 NE2
	2.9	His142 NE2
	3.0	His182 ND1
F1	3.0	Tyr312 OH
	2.9	Pro140 CG
	3.1	Water
F2	3.0	Gly310 amide
	2.9	Asp180 OD2
F3	3.1	Cys153 SG
	3.2	His143 CD2

The fluorogenic HDAC assays and the standard HDAC assays with rat liver HDAC were performed as described previously (Hildmann *et al.*, 2004; Wegener *et al.*, 2003; Riester *et al.*, 2004).

2.2. Synthesis of HDAC inhibitors

All chemicals were purchased from Sigma (Taufkirchen, Germany). Suberoyl anilide hydroxamic acid (SAHA) was synthesized according to standard methods (Bouchain & Delorme, 2003). 9,9,9-Trifluoro-8-oxo-*N*-phenylnonanamide was synthesized by first reacting 100 µmol of the corresponding acid in 500 µl dichloromethane (DCM) with 300 µmol $(COCl)_2$ for 2 h at room temperature. The acyl chloride product mixed with 1 ml DCM was collected after centrifugation and extracted three times with 0.5 ml DCM. Next, a mixture of 0.8 mmol pyridine in 1 ml Et_2O was prepared at 255 K and combined with 0.6 mmol trifluoroacetic anhydride. This mixture was reacted with the acyl chloride for 2 h at room temperature. Products were extracted twice with DCM and the combined extracts were evaporated under reduced pressure. The products were dissolved in a small amount of DMSO and purified by reversed-phase HPLC using a 250 × 10 mm C18 column (Jupiter, Phenomenex, Aschaffenburg, Germany), eluted with methanol and dried *in vacuo*. The product was more than 90% pure with a yield of 60%. LC–MS (ESI) data were used to confirm the expected molecular mass.

3. Results and discussion

3.1. Overall structure

The structure of HDAH bound to the inhibitor 9,9,9-trifluoro-8-oxo-*N*-phenylnonanamide shows only minor differences compared with that of HDAH without inhibitor bound. As observed previously, a Zn ion is found in the active site of HDAH; however, the occupancy of this Zn ion is only 50% (Nielsen *et al.*, 2005). The inhibitor is well defined in the electron density, except for the ring region, which appears to be too flexible to be observed (see Fig. 1). Interestingly, the 9,9,9-trifluoro-8-oxo-*N*-phenylnonanamide inhibitor adopts two conformations in the crystal, where one of the conformations is likely to correspond to the Zn-free enzyme and the other conformation corresponds to the situation where the Zn ion is bound (see Figs. 1 and 2 for representations of the two different conformations). This is based on the observation that the occupancy of the inhibitor is higher than the occupancy of the Zn ion. When setting the occupancy of the inhibitors to the same value as the Zn ion, strong positive electron density above 3σ is found in the $|F_o - F_c|$ map.

Table 3
Inhibition of HDAH and rat liver HDAC by SAHA and 9,9,9-trifluoro-8-oxo-*N*-phenylnonanamide.

	IC_{50} (µ*M*)	
Inhibitor	FB188 HDAH	RL HDAC†
9,9,9-Trifluoro-8-oxo-*N*-phenylnonanamide (Fig. 3*a*)	11.19 ± 2.50	39.66 ± 1.26
SAHA (Fig. 3*b*)	0.95 ± 0.06	0.0096 ± 0.001

† Rat liver HDAC (a mixture containing predominantly HDAC1, 2 and 3; Riester *et al.*, 2004).

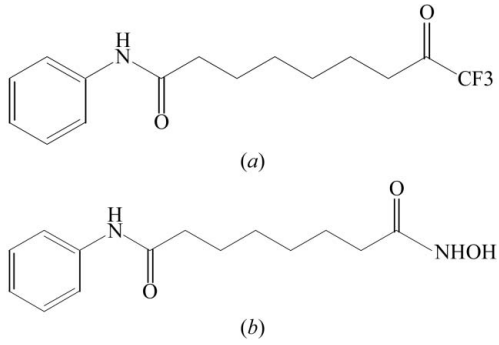

Figure 3
Structures of (*a*) 9,9,9-trifluoro-8-oxo-*N*-phenylnonanamide and (*b*) SAHA.

3.2. Comparison with the SAHA structure

A superposition of the presented structure with the two different conformations of 9,9,9-trifluoro-8-oxo-*N*-phenylnonanamide bound to HDAH and the structure of HDAH with SAHA bound (Nielsen *et al.*, 2005) reveals that the inhibitors bind in similar ways (Fig. 2). The amino acids in the active site from the two different structures superimpose well. The O atom in 9,9,9-trifluoro-8-oxo-*N*-phenylnonanamide in the two different conformations adopts the binding mode of the two O atoms in the head group of SAHA, but slightly displaced (see Fig. 2 and Table 2 for exact distances). Whereas SAHA makes additional contacts with His142, His143 and Tyr312, the 9,9,9-trifluoro-8-oxo-*N*-phenylnonanamide inhibitor complex is stabilized by interactions between the three head-group fluorides and the protein. The amino acids from HDAH involved in the coordination of the inhibitor, the particular atoms and the distances are listed in Table 2. From the superposition in Fig. 2, it is clear that the amino acids in the active site do not undergo major conformational changes upon binding either of the inhibitors; the adaptation of the head group mainly arises from displacement of the water molecules which would otherwise occupy the space. As mentioned, the major differences in the interactions between HDAH and either SAHA or 9,9,9-trifluoro-8-oxo-*N*-phenylnonanamide are found in the head group. The majority of the contacts in the complex between HDAH and 9,9,9-trifluoro-8-oxo-*N*-phenylnonanamide are made to amino acids which are well conserved in both class 1 and class 2 enzymes. However, some exceptions are found. F atom F1 interacts with Tyr312, Pro140 and a well defined water molecule. Pro140 is only conserved in class 2 enzymes but is not found in class 1 enzymes. An inhibitor contact to this amino acid could favour selective binding to class 2 enzymes. Tyr312 and Lys43 coordinate the well defined water molecule. Lys43 is not a conserved amino acid and is often substituted by hydrophobic amino acids in the other enzymes (alignment data not shown), which could make the coordination of the water molecule in the other enzymes weaker.

3.3. Inhibition of FB188 HDAH by SAHA and 9,9,9-trifluoro-8-oxo-*N*-phenylnonanamide

Inhibition of HDAH by SAHA and 9,9,9-trifluoro-8-oxo-*N*-phenylnonanamide was measured in standard fluorogenic HDAC assays as described previously (Hildmann *et al.*, 2004; Riester *et al.*, 2004; Wegener *et al.*, 2003). IC_{50} values are depicted in Table 3. SAHA exhibited a significantly more pronounced specificity for the rat liver enzyme (a mixture containing predominantly HDAC1, 2 and 3; Riester *et al.*, 2004), with an IC_{50} value in the lower nanomolar region, compared with HDAH (IC_{50} = 0.95 μ*M*). In contrast, 9,9,9-trifluoro-8-oxo-*N*-phenylnonanamide showed a slight selectivity for HDAH (IC_{50} = 11.19 μ*M*) compared with the rat liver enzyme (IC_{50} = 39.66 μ*M*). These values are in good agreement with published data for 9,9,9-trifluoro-8-oxo-*N*-phenylnonanamide measured for a partially purified HDAC preparation consisting primarily of HDAC1 and HDAC2 from the nuclear extract of K562 cells (IC_{50} = 6.7 μ*M*; Frey *et al.*, 2002).

3.4. Implications for future drug design

The first structure of a trifluoromethylketone inhibitor in complex with a histone deacetylase-like enzyme not only reveals details of the inhibitor–enzyme interaction, but also provides hints on how to modify existing trifluoromethylketone inhibitors while keeping all existing contacts to the enzyme or even generating new interactions. Possible positions for further derivatization include substitutions of the C atoms following the active-site binding carbonyl. Substitutions at these sites may stabilize the adjacent carbonyl group against metabolic attack, which is known to generate the inactive trifluoromethyl alcohol analogues as major metabolites of trifluoromethyl ketones (Frey *et al.*, 2002; Veale *et al.*, 1997). In this way, metabolic instability as a major drawback of trifluoromethyl ketones could possibly be mitigated.

This work was supported in part by grant BioFuture 0311852 to AS from the Bundesministerium für Forschung und Technologie.

References

Bouchain, G. & Delorme, D. (2003). *Curr. Med. Chem.* **10**, 2359–2372.
Cowan, K. N., Heilbut, A., Humpl, T., Lam, C., Ito, S. & Rabinovitch, M. (2000). *Nature Med.* **6**, 698–702.
DeLano, W. L. (2002). *The PyMOL Molecular Graphics System.* http://www.pymol.org.
Finnin, M. S., Donigian, J. R., Cohen, A., Richon, V. M., Rifkind, R. A., Marks, P. A., Breslow, R. & Pavletich, N. P. (1999). *Nature (London)*, **401**, 188–193.
Frey, R. R., Wada, C. K., Garland, R. B., Curtin, M. L., Michaelides, M. R., Li, J., Pease, L. J., Glaser, K. B., Marcotte, P. A., Bouska, J. J., Murphy, S. S. & Davidsen, S. K. (2002). *Bioorg. Med. Chem. Lett.* **12**, 3443–3447.
Hildmann, C., Ninkovic, M., Dietrich, R., Wegener, D., Riester, D., Zimmermann, T., Birch, O. M., Bernegger, C., Loidl, P. & Schwienhorst, A. (2004). *J. Bacteriol.* **8**, 2328–2339.
Johnstone, R. W. (2002). *Nature Rev.* **1**, 287–299.
Jones, T. A. & Kjeldgaard, M. (1997). *Methods Enzymol.* **277**, 173–208.
Kamita, S. G., Hinton, A. C., Wheelock, C. E., Wogulis, M. D., Wilson, D. K., Wolf, N. M., Stok, J. E., Hock, B. & Hammock, B. D. (2003). *Insect Biochem. Mol. Biol.* **33**, 1261–1273.
Koutek, B., Prestwich, G. D., Howlett, A. C., Chin, S. A., Salehani, D., Akhavan, N. & Deutsch, D. G. (1994). *J. Biol. Chem.* **269**, 22937–22940.
Laskowski, R. A., MacArthur, M. W., Moss, D. S. & Thornton, J. M. (1993). *J. Appl. Cryst.* **26**, 283–291.
Liu, L. T., Chang, H. C., Chiang, L. C. & Hung, W. C. (2003). *Cancer Res.* **63**, 3069–3072.
Marks, P. A., Richon, V. M. & Rifkind, R. A. (2000). *J. Natl Cancer Inst.* **92**, 1210–1206.
Monneret, C. (2005). *Eur. J. Med. Chem.* **40**, 1–13.
Murshudov, G. N., Vagin, A. A. & Dodson, E. J. (1997). *Acta Cryst.* D**53**, 240–255.
Nielsen, T. K., Hildmann, C., Dickmanns, A., Schwienhorst, A. & Ficner, R. (2005). *J. Mol. Biol.* **354**, 107–120.
Qian, D. Z., Kato, Y., Shabbeer, S., Wei, Y., Verheul, H. M. W., Salumbides, B., Sanni, T., Atadja, P. & Pili, R. (2006). *Clin. Cancer Res.* **12**, 634–642.
Riester, D., Wegener, D., Hildmann, C. & Schwienhorst, A. (2004). *Biochem. Biophys. Res. Commun.* **324**, 1116–1123.
Rosato, R. R. & Grant, S. (2003). *Cancer Biol. Ther.* **2**, 30–37.
Schüttelkopf, A. W. & van Aalten, D. M. (2004). *Acta Cryst.* D**60**, 1355–1363.
Somoza, J. R. *et al.* (2004). *Structure*, **12**, 1325–1334.
Vagin, A. & Teplyakov, A. (1997). *J. Appl. Cryst.* **30**, 1022–1025.
Vannini, A., Volpari, C., Filocamo, G., Casavola, E. C., Brunetti, M., Renzoni, D., Chakravarty, P., Paolini, C., De Francesco, R., Gallinari, P., Steinkühler, C. & Di Marco, S. (2004). *Proc. Natl Acad. Sci. USA*, **101**, 15064–15069.
Veale, C. A. *et al.* (1997). *J. Med. Chem.* **40**, 3173–3181.
Villar-Garea, A. & Esteller, M. (2004). *Int. J. Cancer*, **112**, 171–178.
Wada, C. K., Frey, R. R., Curtin, M. L., Garland, R. B., Holms, J. H., Pease, L. J., Guo, J., Glaser, K. B., Marcotte, P. A., Richardson, P. L., Murphy, S. S., Bouska, J. J., Tapang, P., Magoc, T. J., Albert, D. H., Davidsen, S. K. & Michaelides, M. R. (2003). *Bioorg. Med. Chem. Lett.* **13**, 3331–3335.
Wegener, D., Hildmann, C., Riester, D. & Schwienhorst, A. (2003). *Anal. Biochem.* **321**, 202–208.